

International Journal of Modern Physics A
© World Scientific Publishing Company

DISPERSION INTERACTION OF ATOMS WITH SINGLE-WALLED CARBON NANOTUBES DESCRIBED BY THE DIRAC MODEL

YU. V. CHURKIN, A. B. FEDORTSOV, G. L. KLIMCHITSKAYA and V. A. YUROVA
North-West Technical University, Millionnaya Street 5, St.Petersburg, 191065, Russia

Received 2 June 2011
Revised 1 July 2011

We calculate the interaction energy and force between atoms and molecules and single-walled carbon nanotubes described by the Dirac model of graphene. For this purpose the Lifshitz-type formulas adapted for the case of cylindrical geometry with the help of the proximity force approximation are used. The results obtained are compared with those derived from the hydrodynamic model of graphene. Numerical computations are performed for hydrogen atoms and molecules. It is shown that the Dirac model leads to larger values of the van der Waals force than the hydrodynamic model. For a hydrogen molecule the interaction energy and force computed using both models are larger than for a hydrogen atom.

Keywords: Dispersion interaction; carbon nanotube; Dirac model of graphene.

PACS numbers: 12.20.-m, 42.50.Ct, 78.20.Ci

1. Introduction

Dispersion interaction of atoms and molecules with different carbon nanostructures is of topical interest for both fundamental and applied physics. Carbon nanostructures possess unique electrical, mechanical and optical properties¹ leading to a variety of unexpected phenomena. One of them is the possibility to absorb hydrogen atoms and molecules that can be used for hydrogen storage.² Keeping in mind that for technological purposes there is a need to create nanostructures capable of absorbing more than 10 mass percent of hydrogen, various theoretical methods allowing calculation of atom-nanostructure interaction are of much current attention.

In the last few years dispersion interaction between atoms (molecules) and graphene (a single sheet of graphite) and single-walled carbon nanotubes was actively investigated by using the phenomenological density-functional theory.^{3–6} The multiwalled carbon nanotubes with at least several walls can be described by using the concept of the dielectric permittivity of graphite. Because of this, the dispersion interaction between atoms and multiwalled nanotubes can be calculated⁷ using the Lifshitz theory⁸ and the proximity force approximation (PFA) (see Ref. 9 for a review). However, taking into account quick progress in measurements of the van der Waals and Casimir forces,¹⁰ the more fundamental calculation methods of the

dispersion interaction between atoms and single-walled carbon nanotubes are also much needed.

Recent progress allowed generalization of the Lifshitz theory for the material bodies of arbitrary shape with known reflection properties.^{9,11–13} Along these lines the dispersion interaction between carbon nanostructures and material bodies can be described if the reflection properties of the electromagnetic oscillations on graphene are available. In the framework of the so-called *hydrodynamic* model, graphene was considered as an infinitesimally thin positively charged flat sheet, carrying a homogeneous fluid with some mass and negative charge densities.¹⁴ The reflection coefficients of electromagnetic oscillations on such a sheet were found in Refs. 15 and 16. Using these reflection coefficients, the Lifshitz theory was applied to calculate the dispersion interaction between two parallel graphene sheets,¹⁷ between graphene and a material plate,¹⁸ and between graphene and an atom or a molecule.¹⁹ By combining the original formulation of the Lifshitz theory (which is applicable to only plane parallel systems) with the PFA, it was possible also to calculate the dispersion interaction between an atom or a molecule and a single-walled carbon nanotube¹⁹ in the framework of the hydrodynamic model of graphene.

A more exact description of graphene is given by the *Dirac* model^{20–22} which takes into account that the quasiparticle fermion excitations in graphene are the massless Dirac fermions which move with a Fermi velocity and have a linear dispersion relation. This description is also an approximation (it is valid at low energies up to a few eV). Under the assumption that the Dirac model holds at any energy, the reflection coefficients for the electromagnetic oscillations on graphene were found in Ref. 23. The Lifshitz theory combined with the reflection coefficients of the Dirac model has been used to calculate the Casimir interaction between a graphene and a parallel ideal metal plane²³ and between atoms and molecules and graphene.²⁴ The computational results obtained using the hydrodynamic and Dirac models were compared.²⁴ Specifically, an experiment on quantum reflection was proposed²⁴ allowing to discriminate between the predictions of the hydrodynamic and Dirac models of graphene. The influence of the thermal effects in the framework of the Dirac model was investigated in Ref. 25.

In this paper, we calculate the energy and force of dispersion interaction between hydrogen atoms and molecules and single-walled carbon nanotubes using the Dirac model. The obtained results are compared with those obtained earlier using the hydrodynamic model. Keeping in mind that at short separations from 1 to 3 nm, which are most interesting for the investigation of absorption processes, the thermal effects are negligibly small, we consider the Dirac model at zero temperature. We arrive at the conclusion that the van der Waals coefficient of the interaction energy computed using the Dirac model can be both larger and smaller than the same coefficient computed using the hydrodynamic model depending on separation. As to the coefficient of the van der Waals force, it is always larger when the Dirac model is used in computations.

The paper is organized as follows. In Sec. 2 we present the Lifshitz-type formulas

for the atom-nanotube interaction and the reflection coefficients for both models of graphene. Section 3 contains the results of numerical computations of the van der Waals energy and force. In Sec. 4 the reader will find our conclusions and discussion.

2. Energy and Force of Dispersion Interaction Between an Atom and a Nanotube

We use the Lifshitz-type formulas for the van der Waals and Casimir-Polder interaction of atoms (molecules) with single-walled carbon nanotubes obtained using the PFA.^{7,9,19} The validity of the PFA for the configuration of an atom near an ideal-metal cylindrical shell, where the exact expression for the Casimir-Polder potential is available, was recently demonstrated in Ref. 26. Specifically, it was shown²⁶ that for $a/R = 0.1$ (R is the cylinder radius and a is the separation distance between an atom and a cylindrical surface) the relative deviation between the exact and the PFA results is of about 1%. At $a/R = 0.6$ this deviation does not exceed 4%. The same measure of agreement between the exact and the PFA results for atom-cylinder interaction is expected for cylinders made of real materials.

The Lifshitz-type formulas for the interaction energy and force between an atom (molecule) and a single-walled nanotube in the framework of the PFA are given by

$$\begin{aligned}
 E(a) &= -\frac{\hbar}{2\pi} \sqrt{\frac{R}{R+a}} \int_0^\infty d\xi \alpha(i\xi) \int_0^\infty k dk e^{-2aq} \\
 &\quad \times \left[q - \frac{1}{4(R+a)} \right] \left[2r_{\text{TM}} - \frac{\xi^2}{q^2 c^2} (r_{\text{TM}} + r_{\text{TE}}) \right], \quad (1) \\
 F(a) &= -\frac{\hbar}{2\pi} \sqrt{\frac{R}{R+a}} \int_0^\infty d\xi \alpha(i\xi) \int_0^\infty k dk e^{-2aq} \\
 &\quad \times \left[2q^2 - \frac{3}{8(R+a)^2} \right] \left[2r_{\text{TM}} - \frac{\xi^2}{q^2 c^2} (r_{\text{TM}} + r_{\text{TE}}) \right].
 \end{aligned}$$

Here, $\alpha(\omega)$ is the dynamic polarizability of an atom or a molecule, $\omega = i\xi$ is the imaginary frequency, $q^2 = k^2 + \xi^2/c^2$, and r_{TM} and r_{TE} are the reflection coefficients of the electromagnetic fluctuations on graphene for two independent polarizations of the electromagnetic field, transverse magnetic and transverse electric.

The explicit expressions for the reflection coefficients depend on the model of the electronic structure of graphene used. In the framework of the Dirac model these coefficients can be presented in the form²³

$$\begin{aligned}
 r_{\text{TM}} &\equiv r_{\text{TM}}^{(D)}(i\xi, k) = \frac{\alpha q \Phi(\tilde{q})}{2\tilde{q}^2 + \alpha q \Phi(\tilde{q})}, \\
 r_{\text{TE}} &\equiv r_{\text{TE}}^{(D)}(i\xi, k) = -\frac{\alpha \Phi(\tilde{q})}{2q + \alpha \Phi(\tilde{q})}, \quad (2)
 \end{aligned}$$

where $\alpha = e^2/(\hbar c) \approx 1/137$ is the fine-structure constant, $\tilde{q}^2 = (v_{\text{F}}^2 k^2 + \xi^2)/c^2$, $v_{\text{F}} \approx 10^6$ m/s is the Fermi velocity, and the function Φ determines the polarization tensor in an external electromagnetic field in the one-loop approximation in

4 *Yu. V. Churkin et al.*

three dimensional space-time. The explicit form of this function along the imaginary frequency axis is the following:²³

$$\Phi(\tilde{q}) = N \left(\tilde{\Delta} + \frac{\tilde{q}^2 - 4\tilde{\Delta}^2}{2\tilde{q}} \arctan \frac{\tilde{q}}{2\tilde{\Delta}} \right). \quad (3)$$

Here, $N = 4$, $\tilde{\Delta} = \Delta/(\hbar c)$, and the exact value of the gap parameter Δ remains unknown. The upper bound on Δ is equal to about 0.1 eV, but the true value of Δ might be much smaller.²²

In the framework of the hydrodynamic model the reflection coefficients are presented differently

$$\begin{aligned} r_{\text{TM}} &\equiv r_{\text{TM}}^{(h)}(i\xi, k) = \frac{c^2 q K}{c^2 q K + \xi^2}, \\ r_{\text{TE}} &\equiv r_{\text{TE}}^{(h)}(i\xi, k) = -\frac{K}{K + q}, \end{aligned} \quad (4)$$

where the wave number of the graphene sheet $K = 6.75 \times 10^5 \text{ m}^{-1}$ corresponds to the frequency $\omega_K = cK = 2.02 \times 10^{14} \text{ rad/s}$.

For the purposes of numerical computations it is convenient to introduce the separation-dependent van der Waals coefficient $C_3(a)$ and the force coefficient $C_F(a)$, so that the interaction energy and force (1) are represented as

$$E(a) = -\frac{C_3(a)}{a^3}, \quad F(a) = -\frac{C_F(a)}{a^4}. \quad (5)$$

The explicit form of the coefficients $C_3(a)$ and $C_F(a)$ in terms of dimensionless variable $y = 2aq$ is obtained from Eq. (1)

$$\begin{aligned} C_3(a) &= \frac{\hbar}{16\pi} \sqrt{\frac{R}{R+a}} \int_0^\infty d\xi \alpha(i\xi) \int_{2a\xi/c}^\infty y dy e^{-y} \\ &\quad \times \left[y - \frac{a}{2(R+a)} \right] \left[2r_{\text{TM}} - \frac{4a^2 \xi^2}{y^2 c^2} (r_{\text{TM}} + r_{\text{TE}}) \right], \\ C_F(a) &= \frac{\hbar}{16\pi} \sqrt{\frac{R}{R+a}} \int_0^\infty d\xi \alpha(i\xi) \int_{2a\xi/c}^\infty y dy e^{-y} \\ &\quad \times \left[y^2 - \frac{3a^2}{4(R+a)^2} \right] \left[2r_{\text{TM}} - \frac{4a^2 \xi^2}{y^2 c^2} (r_{\text{TM}} + r_{\text{TE}}) \right]. \end{aligned} \quad (6)$$

Equations (5) and (6) can be used with either the Dirac- or hydrodynamic-model reflection coefficients taking into account that in terms of the variable y it holds

$$q = \frac{y}{2a}, \quad \tilde{q} = \left[\frac{v_{\text{F}}^2}{c^2} \frac{y^2}{4a^2} + \left(1 - \frac{v_{\text{F}}^2}{c^2} \right) \frac{\xi^2}{c^2} \right]^{1/2}. \quad (7)$$

For an atom interacting with a graphene sheet the interaction energy also has the form of Eq. (5), but the van der Waals coefficient is given by²⁴

$$C_3(a) = \frac{\hbar}{16\pi} \int_0^\infty d\xi \alpha(i\xi) \int_{2a\xi/c}^\infty dy e^{-y} \times \left[2y^2 r_{\text{TM}} - \frac{4a^2 \xi^2}{c^2} (r_{\text{TM}} + r_{\text{TE}}) \right]. \quad (8)$$

Note that if the coefficient C_3 would not depend on a and the equality $C_F = 3C_3$ be satisfied, then Eq. (5) describes the nonretarded van der Waals interaction between an atom and a material wall.^{8–10,27–30} Numerical computations performed in the next section show that for hydrogen atoms and molecules interacting with a graphene sheet and single-walled carbon nanotubes the coefficients C_3 and C_F are separation-dependent down to the shortest separation distances of about 1 nm where a macroscopic description of dispersion interaction by means of the Lifshitz-type formulas remains applicable.

3. Dispersion Interaction of Hydrogen Atoms and Molecules with Single-Walled Carbon Nanotubes

In this section, we perform numerical computations of the coefficients C_3 and C_F in Eq. (6) describing the energy and force of the van der Waals interaction, respectively. All computations are performed for hydrogen atoms and molecules using the Dirac and hydrodynamic models of graphene, and the obtained results are compared. The atomic and molecular dynamic polarizabilities of hydrogen can be represented with sufficient precision using the single-oscillator model.^{7,30} According to this model, the dynamic polarizabilities along the imaginary frequency axis take the form

$$\alpha(i\xi) = \frac{\alpha(0)}{1 + \frac{\xi^2}{\omega_0^2}}, \quad (9)$$

where $\alpha(0)$ is the static atomic (molecular) polarizability and ω_0 is the characteristic frequency. For a hydrogen atom it was found³¹ that $\alpha(0) \equiv \alpha_a(0) = 4.50$ a.u. (1 a.u. of polarizability is equal to $1.482 \times 10^{-31} \text{ m}^3$) and $\omega_0 \equiv \omega_{0a} = 11.65$ eV. For a hydrogen molecule³¹ $\alpha(0) \equiv \alpha_m(0) = 5.439$ a.u. and $\omega_0 \equiv \omega_{0m} = 14.09$ eV.

In Fig. 1(a) we present the computational results for the van der Waals coefficient $C_{3,\text{H}}$ in atomic units as a function of separation for the interaction of a hydrogen atom (the dashed and solid lines labeled 1) and molecule (the dashed and solid lines labeled 2) with graphene. One atomic unit for C_3 is equal to $4.032 \times 10^{-3} \text{ eV nm}^3$. The solid lines 1 and 2 are computed using the Dirac model (2) with the gap parameter $\Delta = 0.1$ eV (as shown in Ref. 24, the computational results only slightly depend on the value of Δ). The dashed lines 1 and 2 are computed using the hydrodynamic model (4). Figure 1(a) extends the results of Ref. 24 for separations below 3 nm. At $a > 3$ nm the van der Waals coefficient $C_3^{(h)}$ computed using the hydrodynamic model is always larger than $C_3^{(D)}$ computed using the Dirac model.²⁴

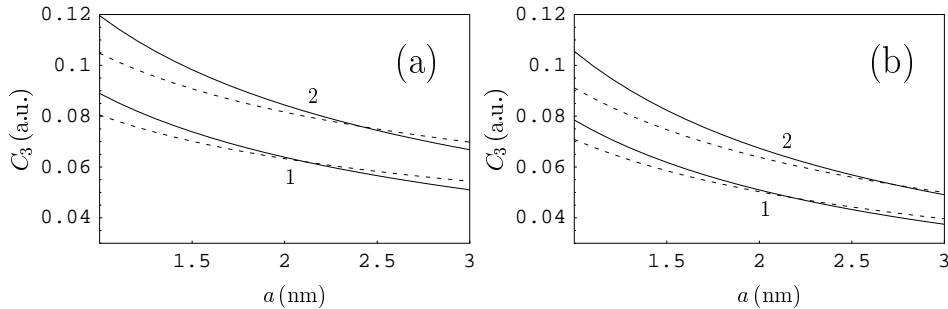


Fig. 1. The van der Waals coefficients for hydrogen atom (the solid and dashed lines labeled 1) and molecule (the solid and dashed lines labeled 2) interacting with (a) a graphene sheet and (b) a single-walled carbon nanotube of $R = 5$ nm radius as a function of separation. Computations are performed using the Dirac (the solid lines) and hydrodynamic (the dashed lines) models of graphene.

As can be seen in Fig. 1(a), at $a < 3$ nm this is, however, not so. Thus, for hydrogen atom at $a < 2.1$ nm $C_3^{(h)} < C_3^{(D)}$. For hydrogen molecule the same holds at $a < 2.42$ nm.

In Fig. 1(b) similar results are shown for hydrogen atom and molecule interacting with the single-walled carbon nanotube of 5 nm radius. All notations are the same as in Fig. 1(a). The maximum separation distance $a = 3$ nm is chosen in order to preserve the parameter $a/R \leq 0.6$, i.e., to avoid large deviations from the PFA. As is seen in Fig. 1(b), for single-walled carbon nanotubes there are also some small separation distances ($a = 2.2$ nm for a hydrogen atom and $a = 2.77$ nm for a hydrogen molecule) where the values of the van der Waals coefficients computed using the Dirac and hydrodynamic model become equal.

Now we compute the coefficient of the van der Waals force C_F in Eq. (6) for an atom and a molecule interacting with a single-walled carbon nanotube. The computational results as a function of separation are presented in Fig. 2(a) for a hydrogen atom and in Fig. 2(b) for a hydrogen molecule. In both cases the nanotube radius is $R = 5$ nm. As can be seen in Fig. 2(a,b), independently of the model of graphene used (the solid lines are for the Dirac model with the gap parameter $\Delta = 0.1$ eV and the dashed lines are for the hydrodynamic model), C_F is the monotonously decreasing function with the increase of separation. The largest relative differences between the values of C_F computed using the Dirac and the hydrodynamic model (29% for a hydrogen atom and 30% for a hydrogen molecule) are achieved at $a = 1$ nm.

Further we investigate the dependence of the coefficient C_F in Eq. (6) on the radius of a single-walled carbon nanotube R . In Fig. 3(a) we plot the coefficient C_F as a function of R for the dispersion interaction of a hydrogen atom separated by the distance $a = 1$ nm from the surface of a carbon nanotube. The solid line is obtained by using the reflection coefficients (2) of the Dirac model while the dashed line is

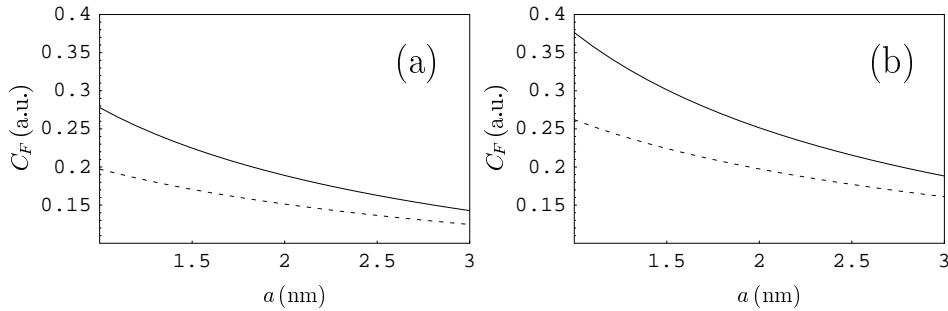


Fig. 2. The coefficients of the van der Waals force for hydrogen (a) atom and (b) molecule interacting with a single-walled carbon nanotube of $R = 5$ nm radius as a function of separation. Computations are performed using the Dirac (the solid lines) and hydrodynamic (the dashed lines) models of graphene.

computed with the help of reflection coefficients (4) of the hydrodynamic model. As can be seen in Fig. 3(a), in both models the coefficient C_F slowly increases with increasing radius of the nanotube. For all radii, the value of C_F computed within the Dirac model is larger than within the hydrodynamic model. For example, for a nanotube with $R = 2$ nm the relative difference between the predictions of the Dirac and hydrodynamic models is equal to approximately 30%. Thus, it is several times larger than the error arising from using the PFA (see Sec. 2). In Fig. 3(b) the coefficient C_F as a function of nanotube radius is plotted for a hydrogen molecule at the separation $a = 1$ nm from a single-walled carbon nanotube. The same notations, as in Fig. 3(a), are used. Here, for a nanotube of $R = 2$ nm radius the relative difference between the predictions of the Dirac and hydrodynamic models is equal to 29%. From Fig. 3 it follows that there is only a minor dependence of the

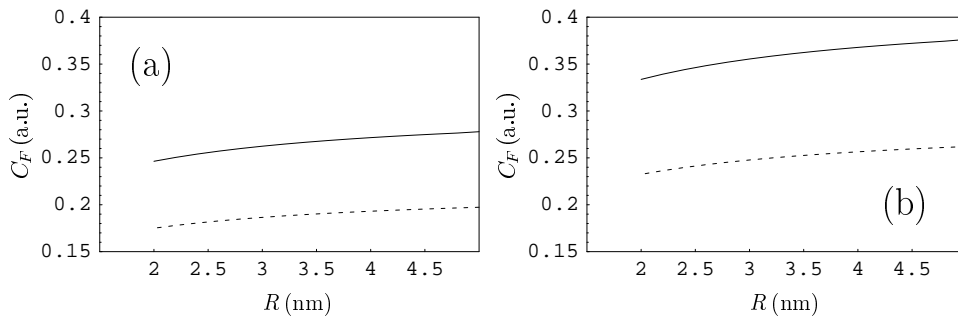


Fig. 3. The coefficients of the van der Waals force for hydrogen (a) atom and (b) molecule interacting with a single-walled carbon nanotube as a function of its radius. Computations are performed using the Dirac (the solid lines) and hydrodynamic (the dashed lines) models of graphene for an atom or a molecule at the separation $a = 1$ nm from the nanotube surface.

relative difference in the predictions of the Dirac and hydrodynamic models for the coefficients C_3 and C_F on a nanotube radius.

4. Conclusions and Discussion

In the foregoing we have investigated the dispersion interaction of hydrogen atoms and molecules with single-walled carbon nanotubes described by the Dirac and hydrodynamic models. The theoretical basis for our study is the Lifshitz theory expressing the interaction energy and force between planar material structures in terms of the reflection coefficients of electromagnetic fluctuations. Using the PFA, the Lifshitz formulas for the van der Waals energy and force were adapted for the configuration of an atom or a molecule interacting with a nanotube of cylindrical shape.

Computations of the van der Waals coefficient C_3 performed in the paper demonstrated that its magnitude for a hydrogen molecule is always significantly larger than for a hydrogen atom. At the same time, the value of C_3 for an atom-graphene (molecule-graphene) interaction is only slightly larger than for an atom-nanotube (molecule-nanotube) interaction. Different models of graphene (Dirac and hydrodynamic) lead to a bit different predictions for C_3 as a function of separation. Furthermore, there is the separation distance below 3 nm where both models result in one and the same value of C_3 .

Similar results follow from computations of the coefficient C_F characterizing the van der Waals force. Its magnitude for a hydrogen molecule is also significantly larger than for a hydrogen atom. It is interesting that the Dirac model of graphene leads to markedly larger results for C_F than the hydrodynamic model. In the application region of the PFA, there is no separation distance where the values of C_F predicted by the two models would be equal. We demonstrated that the above results are preserved for single-walled carbon nanotubes of different radii from 2 to 5 nm. Keeping in mind that the Dirac model gives a more accurate description of graphene at low energies than the hydrodynamic model, the former can be applied to calculate the capacity of single-walled carbon nanotubes to absorb hydrogen atoms and molecules for use in hydrogen storage.

Acknowledgments

This work was supported by the Grant of the Russian Ministry of Education P-184.

References

1. P. J. F. Harris, *Carbon Nanotubes and Related Structures: New Materials for the Twenty-First Century* (Cambridge University Press, New York, 1999).
2. Yu. S. Nechaev, *Usp. Fis. Nauk* **176**, 581 (2006) [*Phys. Uspekhi* **49**, 563 (2006)].
3. A. Bogicevic, S. Ovesson, P. Hyldgaard, B. I. Lundqvist, H. Brune and D. R. Jennison, *Phys. Rev. Lett.* **85**, 1910 (2000).

4. E. Hult, P. Hyldgaard, J. Rossmeisl and B. I. Lundqvist, *Phys. Rev. B* **64**, 195414 (2001).
5. J. Jung, P. García-González, J. F. Dobson and R. W. Godby, *Phys. Rev. B* **70**, 205107 (2004).
6. J. F. Dobson, A. White and A. Rubio, *Phys. Rev. Lett.* **96**, 073201 (2006).
7. E. V. Blagov, G. L. Klimchitskaya and V. M. Mostepanenko, *Phys. Rev. B* **71**, 235401 (2005).
8. E. M. Lifshitz and L. P. Pitaevskii, *Statistical Physics*, Pt.II (Pergamon, Oxford, 1984).
9. M. Bordag, G. L. Klimchitskaya, U. Mohideen and V. M. Mostepanenko, *Advances in the Casimir Effect* (Oxford University Press, Oxford, 2009).
10. G. L. Klimchitskaya, U. Mohideen and V. M. Mostepanenko, *Rev. Mod. Phys.* **81**, 1827 (2009).
11. T. Emig, R. L. Jaffe, M. Kardar and A. Scardicchio, *Phys. Rev. Lett.* **96**, 080403 (2006).
12. M. Bordag, *Phys. Rev. D* **73**, 125018 (2006).
13. O. Kenneth and I. Klich, *Phys. Rev. Lett.* **97**, 160401 (2006).
14. A. L. Fetter, *Ann. Phys. (N.Y.)* **81**, 367 (1973).
15. G. Barton, *J. Phys. A* **37**, 1011 (2004).
16. G. Barton, *J. Phys. A* **38**, 2997 (2005).
17. M. Bordag, *J. Phys. A* **39**, 6173 (2006).
18. M. Bordag, B. Geyer, G. L. Klimchitskaya and V. M. Mostepanenko, *Phys. Rev. B* **74**, 205431 (2006).
19. E. V. Blagov, G. L. Klimchitskaya and V. M. Mostepanenko, *Phys. Rev. B* **75**, 235413 (2007).
20. G. W. Semenoff, *Phys. Rev. Lett.* **53**, 2449 (1984).
21. D. P. DiVincenzo and E. J. Mele, *Phys. Rev. B* **29**, 1685 (1984).
22. A. H. Castro-Neto, F. Guinea, N. M. R. Peres, K. S. Novoselov and A. K. Geim, *Rev. Mod. Phys.* **81**, 109 (2009).
23. M. Bordag, I. V. Fialkovsky, D. M. Gitman and D. V. Vassilevich, *Phys. Rev. B* **80**, 245406 (2009).
24. Yu. V. Churkin, A. B. Fedortsov, G. L. Klimchitskaya and V. A. Yurova, *Phys. Rev. B* **82**, 165433 (2010).
25. I. V. Fialkovsky, V. N. Marachevsky and D. V. Vassilevich. Finite temperature Casimir effect for graphene, e-print arXiv:1102.1757v1.
26. V. B. Bezerra, E. R. Bezerra de Mello, G. L. Klimchitskaya, V. M. Mostepanenko and A. A. Saharian, *Eur. Phys. J. C* **71**, 1614 (2011).
27. J. Mahanty and B. W. Ninham, *Dispersion Forces* (Academic Press, London, 1976).
28. V. A. Parsegian, *Van der Waals Forces: A Handbook for Biologists, Chemists, Engineers, and Physicists* (Cambridge University Press, Cambridge, 2005).
29. J. F. Babb, G. L. Klimchitskaya and V. M. Mostepanenko, *Phys. Rev. A* **70**, 042901 (2004).
30. A. O. Caride, G. L. Klimchitskaya, V. M. Mostepanenko and S. I. Zanette, *Phys. Rev. A* **71**, 042901 (2005).
31. A. Rauber, J. R. Klein, M. W. Cole and L. W. Bruch, *Surf. Sci.* **123**, 173 (1982).